Overexpression of adrenomedullin protects mesenchymal stem cells against hypoxia and serum deprivation-induced apoptosis via the Akt/GSK3β and Bcl-2 signaling pathways

HONGJIN SI[1,2*], YAO ZHANG[1,2*], YUQING SONG[1,2] and LILI LI[1,2]

[1]The Key Laboratory of Myocardial Ischemia, Harbin Medical University, Ministry of Education;
[2]Department of Cardiology, The Second Affiliated Hospital of Harbin Medical University, Harbin, Heilongjiang 150086, P.R. China

Received October 7, 2016; Accepted February 2, 2018

DOI: 10.3892/ijmm.2018.3533

Abstract. The poor survival rate of transplanted mesenchymal stem cells (MSCs) within the ischemic heart limits their therapeutic potential for cardiac repair. Adrenomedullin (ADM) has been identified as a potent apoptotic inhibitor. The present study aimed to investigate the protective effects of ADM on MSCs against hypoxia and serum deprivation (H/SD)-induced apoptosis, and to determine the potential underlying mechanisms. In the present study, a recombinant adenovirus expressing the ADM gene was established and was infected into MSCs. The infection rate was determined via microscopic detection of green fluorescence and flow cytometric analysis. The mRNA expression levels of ADM were detected by reverse transcription-polymerase chain reaction. In addition, a model of H/SD was generated. The MSCs were randomly separated into six groups: Control, enhanced green fluorescent protein (EGFP)-Adv, EGFP-ADM, H/SD, EGFP-Adv + H/SD and EGFP-ADM + H/SD. Cell viability and proliferation were determined using the Cell Counting kit-8 assay. Apoptosis was assessed by terminal deoxynucleotidyl transferase-mediated-dUTP nick-end labeling assay and flow cytometric analysis using Annexin V-phycoerythrin/7-aminoactinomycin D staining. The protein expression levels of total protein kinase B (Akt), phosphorylated (p)-Akt, total glycogen synthase kinase (GSK)3β, p-GSK3β, B-cell lymphoma 2 (Bcl-2), Bcl-2-associated X protein (Bax), caspase-3 and cleaved caspase-3 were detected by western blot analysis. The results indicated that ADM overexpression could improve MSC proliferation and viability, and protect MSCs against H/SD-induced apoptosis. In addition, ADM overexpression increased Akt and GSK3β phosphorylation, and Bcl-2/Bax ratio, and decreased the activation of caspase-3. These results suggested that ADM protects MSCs against H/SD-induced apoptosis, which may be mediated via the Akt/GSK3β and Bcl-2 signaling pathways.

Correspondence to: Dr Lili Li, Department of Cardiology, The Second Affiliated Hospital of Harbin Medical University, 148 Baojian Road, Harbin, Heilongjiang 150086, P.R. China
E-mail: lisister1980@163.com

*Contributed equally

Key words: adrenomedullin, mesenchymal stem cells, apoptosis, hypoxia and serum deprivation, Akt/GSK3β pathway, Bcl-2 pathway

Introduction

Mesenchymal stem cells (MSCs) have exhibited potential for the treatment of ischemic heart diseases. Previous studies demonstrated that MSCs derived from the bone marrow can differentiate into cardiac myocytes *in vitro* and *in vivo* (1-3). Furthermore, it has been reported that MSCs transplanted into the acute ischemic heart and chronic congestive heart may modify cardiac function by promoting angiogenesis and reducing myocardial fibrosis (4-6). However, the therapeutic potential of MSCs is limited by their low survival rate following transplantation into damaged myocardium (7,8). A previous study revealed that <1% of MSCs were detected 24 h following transplantation into a rat heart with experimental myocardial infarction (MI) (9). Cell apoptosis, which is caused by the harsh hypoxic microenvironment, contributes to the low survival rate of transplanted MSCs (10,11). Therefore, the present study aimed to protect MSCs against apoptosis, in order to improve the therapeutic efficacy of MSCs transplantation.

Adrenomedullin (ADM) is a ubiquitous peptide synthesized by numerous cell types, including neurons, macrophages, monocytes, lymphocytes, and epithelial and endothelial cells (12-14). Although ADM was initially described as a potent vasodilator and hypotensive factor, numerous studies have reported that it may induce various biological activities in a paracrine or autocrine manner. It has been reported that ADM is not only able to enhance cell proliferation and angiogenesis (15-17), but can inhibit cell apoptosis (18). Furthermore, it has been demonstrated that ADM protects numerous cell types, including cardiomyocytes (19), rat Leydig cells (20), endothelial progenitor cells (21) and vascular endothelial cells (22), against apoptosis via the protein kinase B (Akt)/glycogen synthase kinase (GSK)3β signaling pathway.

Akt is a powerful survival signal, which suppresses apoptosis and increases cell survival. Activation of Akt can trigger GSK3β phosphorylation (23), which subsequently results in an antiapoptotic effect via inactivation of caspase-3 (24,25). Furthermore, Akt has been reported to serve an important role in regulating B-cell lymphoma 2 (Bcl-2) family members (26). The Bcl-2 family members are important regulators of mitochondria-mediated apoptosis, and can be divided into anti-apoptotic proteins, such as Bcl-2, and proapoptotic proteins, including Bcl-2-associated X protein (Bax). The Bcl-2/Bax ratio is often used to determine the extent of apoptosis (27). Since the Akt signaling pathway has also been reported to serve an important role in mediating survival signaling in MSCs (28), the present study infected MSCs with ADM, and investigated whether ADM overexpression could protect MSCs from hypoxia and serum deprivation (H/SD)-induced apoptosis via the Akt/GSK3β and Bcl-2 signaling pathways.

Materials and methods

Culture and identification of MSCs. MSCs were isolated from the bone marrow of Sprague-Dawley rats (age, 4 weeks; weight, 60-80 g) according to a previously published method (29,30). Rats were obtained from the Laboratory Animal Science Department, The Second Affiliated Hospital of Harbin Medical University (Harbin, China). The rats were housed at a temperature of 22˚C with a relative humidity of 40-70% and a 12-h light/dark cycle with food/water *ad libitum*. The present study was approved by the Local Ethics Committee for the Care and Use of Laboratory Animals of Harbin Medical University. Briefly, the femurs and tibias were removed from the rats, and the bone marrow was flushed out using 10 ml Dulbecco's modified Eagle's medium/F12 (DMEM/F12; HyClone; GE Healthcare, Logan, UT, USA) supplemented with 1% penicillin/streptomycin (Beyotime Institute of Biotechnology, Nantong, China). Following centrifugation at 1,000 x g at room temperature for 5 min, the resulting cell pellets were resuspended in 6 ml DMEM/F12 supplemented with 10% fetal bovine serum (FBS; ScienCell Research Laboratories, Inc., San Diego, CA, USA) and 1% penicillin/streptomycin, and were plated in a 25 cm^2 plastic flask at 37˚C in a humidified atmosphere containing 5% CO_2 and 95% air. After a 48 h culture, the medium was replaced and non-adherent hematopoietic cells were removed. The remaining spindle-shaped, adherent cells were MSCs. These adherent MSCs were subsequently cultured; the culture medium was regularly changed every 3-4 days. A total of 7-10 days after seeding, the cells became 80-90% confluent. The adherent cells were released from the flask using 0.25% trypsin (Beyotime Institute of Biotechnology) and were expanded at a 1:2 or 1:3 dilution. A total of 9 Sprague-Dawley rats were used in the present study. For each primary cell culture, the bone marrow of 3 rats was mixed together. Passage 2 MSCs were cryopreserved and passage 3-4 MSCs were used in the present study. Primary cell culture was conducted three times, and cells in each primary culture were repeatedly used for subsequent experiments.

To investigate the expression of typical MSC-associated cell surface antigens, MSCs were analyzed by fluorescence-activated cell sorting (FACS). Briefly, MSCs were trypsinized and $1x10^6$ MSCs were incubated with 10 μg antibodies in 1 ml PBS at room temperature in the dark for 15 min. The antibodies used in the present study were as follows: Hematopoietic progenitor marker phycoerythrin (PE)-conjugated mouse anti-rat cluster of differentiation (CD)34 (1:200; sc-74499; Santa Cruz Biotechnology, Inc., Dallas, TX, USA), the pan-leukocyte marker fluorescein isothiocyanate (FITC)-conjugated mouse anti-rat CD45 (1:100; MA5-17385; Caltag Laboratories, Inc., Burlingame, CA, USA), and the MSC marker PE-conjugated anti-rat CD29 (1:100; 102207; BioLegend, Inc., San Diego, CA, USA). To investigate differentiative ability, according to our previous study, MSCs were incubated with osteogenic induction medium (RAWMD-90021; Cyagen Biosciences, Santa Clara, CA, USA) or adipogenic induction medium (RAWMD-90021; Cyagen Biosciences) for 3 or 4 weeks. Subsequently, the cells were stained with von Kossa or Oil Red O (31). The staining results were observed by optical microscope.

Adenoviral transduction of MSCs. The MSCs were transduced with a recombinant adenoviral vector encoding the gene green fluorescent protein (Ad-CMV-GFP). For infection, MSCs were seeded in 6-well plates at $1x10^5$ cells/well and were allowed to grow overnight to 50-60% confluence. Subsequently, the MSCs were infected with enhanced (E) GFP-recombinant adenovirus capsids (EGFP-Adv) or EGFP-recombinant adenovirus capsids containing ADM cDNA (EGFP-ADM) (BC061775; Shanghai GeneChem Co. Ltd., Shanghai, China) at a multiplicity of infection (MOI) of 80 at 37˚C. After 12 h, the medium was replaced with normal medium containing 10% FBS and antibiotics. To confirm infection was successful, the mRNA expression levels of ADM were detected by reverse transcription-polymerase chain reaction (RT-PCR). Briefly, 24, 48 and 72 h post-infection, total RNA was isolated from the MSCs using TRIzol® reagent (Invitrogen; Thermo Fisher Scientific, Inc., Waltham, MA, USA). The β-actin gene was used as a normalizing control. The designed paired primers were as follows: ADM, forward 5'-GGACTTTGCGGGTTTTGC-3', reverse 5'-TCTGGCGGTAGCGTTTGA-3'; and β-actin, forward 5'-ATATCGCTGCGCTCGTCGTC-3' and reverse 5'-GCATCGGAACCGCTCATTGC-3'. PCR conditions were as follows: 25 cycles of denaturation at 94˚C for 30 sec, annealing at 55˚C for 30 sec and extension at 72˚C for 1 min (initial denaturation at 94˚C for 5 min; final extension is 72˚C for 5 min). The PCR products were subjected to 1.5% agarose gel electrophoresis, and were scanned and semi-quantified using ImageQuant software (TL 7.0; GE Healthcare, Chicago, IL, USA). Based on these results, 48 h post-infection, the MSCs were used for subsequent experiments. Furthermore, 48 h post-infection, the infection rate was also assessed by fluorescence microscopy (DMI4000B; Leica Microsystems GmbH, Wetzlar, Germany) and FACS analysis with FACSDiva software (version 4.1; BD Biosciences, Franklin Lakes, NJ, USA). For FACS analysis, the MSCs at 48 h post-infection were digested and centrifuged at 1,000 x g for 5 min. After removing the supernatant, 500 μl PBS buffer was added and the MSCs were analyzed by flow cytometry.

H/SD model and cell groups. MSCs were randomly separated into the following six groups: Control, EGFP-Adv, EGFP-ADM, H/SD, EGFP-Adv + H/SD, and EGFP-ADM + H/SD.

To mimic the *in vivo* ischemic microenvironment, cells were cultured under H/SD conditions, according to a previous study (10). Briefly, 48 h post-infection, the cells in the EGFP-Adv + H/SD, EGFP-ADM + H/SD and H/SD groups were washed with PBS, cultured in serum-free medium and incubated in a glove box (855-AC; Plas-Labs, Inc., Lansing, MI, USA) to scavenge free oxygen at 37˚C for an additional 12 h. The cells in the control, EGFP-Adv and EGFP-ADM groups were cultured in complete medium in a general cell incubator for 12 h. Subsequently, the following experiments were conducted.

Cell viability assay. The viability of MSCs was assessed using the Cell Counting kit-8 assay kit (CCK-8; Dojindo Molecular Technologies, Inc., Kumamoto, Japan) according to the manufacturer's protocol. Cells were seeded into a 96-well plate (5,000 cells/well) after being subjected to the aforementioned experimental treatments, and cell viability was measured following the addition of 10 μl CCK-8 into the culture medium for 1.5 h at 37˚C. The absorbance of each well was quantified at 450 nm. The mean optical density (OD) of 5 wells in each group was used to calculate the percentage of cell viability. The experiments were conducted in triplicate.

Terminal deoxynucleotidyl transferase-mediated-dUTP nick-end labeling (TUNEL) staining. Apoptosis of MSCs was determined using a TUNEL assay (Roche Applied Science, Penzberg, Germany) according to the manufacturer's protocol with some modifications. Briefly, the MSCs were grown in a 24-well plate. Following the aforementioned experimental treatments, the cells were fixed in 4% paraformaldehyde for 1 h at room temperature. Subsequently, the cells ($1x10^5$ cells/well) were incubated with 3% H_2O_2 in methanol for 10 min at room temperature to block endogenous peroxidase activity, and were then incubated with 0.1% Triton X-100 in 0.1% sodium citrate for 2 min at 4˚C. After washing in PBS, the cells were finally incubated with the TUNEL reaction mixture containing 5 μl enzyme solution and 45 μl fluorochrome-labeled solution at 37˚C for 60 min in the dark. For counterstaining, the cells were incubated with DAPI (Beyotime Institute of Biotechnology) for 15 min. The cells were observed using a fluorescence microscope, in which 10 fields were randomly selected. The $TUNEL^+$ and $DAPI^+$ nuclei in the cells were counted manually. The percentage of positive cells was calculated as the apoptotic index (AI) using the following equation: AI = (number of positive cells/total number of cells) x 100%, as previously described (32,33). The experiments were conducted in triplicate.

Flow cytometric analysis of cell apoptosis. Apoptosis of MSCs was also determined by detecting phosphatidylserine exposure on cell plasma membranes using the fluorescent dye Annexin V-PE/7-aminoactinomycin D (7-AAD) apoptosis detection kit (BD Biosciences, San Diego, CA, USA) according to the manufacturer's protocol. This assay is used to discriminate between intact (Annexin V^-/7-AAD^-), early apoptotic (Annexin V^+/7-AAD^-), late apoptotic (Annexin V^+/7-AAD^+) and necrotic cells (Annexin V^-/7-AAD^+). Briefly, at the end of the treatment period, the cells were harvested with 0.25% trypsin and washed twice with cold PBS. After being resuspended in 100 μl 1X binding buffer, 5 μl Annexin V-PE and 5 μl 7-AAD were added, and the cells ($4-5x10^5$ cells) were incubated for 15 min at room temperature in the dark. Finally, 400 μl 1X binding buffer was added to the cells and flow cytometric analysis was conducted. The experiments were conducted in triplicate.

Protein extraction and western blot analysis. After washing with PBS twice, the treated cells were harvested and lysed in ice-cold radioimmunoprecipitation assay lysis buffer (Beyotime Institute of Biotechnology) mixed with protease and phosphatase inhibitors (Roche Applied Science). Total protein in the supernatant was quantified using a bicinchoninic acid protein assay kit (Beyotime Institute of Biotechnology). Equal amounts of protein (50 μg/lane) were separated by 12% SDS-PAGE and were transferred to polyvinylidene fluoride membranes. The membranes were then incubated at room temperature in a blocking solution composed of 5% skim milk powder dissolved in 1X TBS for 1 h at room temperature. Subsequently, the membranes were incubated with the following primary antibodies at 4˚C overnight: Rabbit polyclonal antibodies against Bax (WL01637), Bcl-2 (WL01556), Akt (WL0003b) and GSK3β (WL01456) (all from Wanleibio Co., Ltd., Shanghai, China), rabbit polyclonal antibody against phosphorylated (p)-Akt (Ser-473) (sc-7985-R; Santa Cruz Biotechnology, Inc.), rabbit monoclonal antibody against p-GSK3β (Ser-9, 9322s), rabbit polyclonal antibody against caspase-3 (9662s) (both from Cell Signaling Technology, Inc., Danvers, MA, USA) and mouse polyclonal antibody against GAPDH (KC-5G4; Kangchen Bio-Tech Co., Ltd., Shanghai, China). The membrane was then washed three times with TBS-0.1% Tween (TBST) for 5 min followed by incubation with horseradish peroxidase-conjugated anti-mouse (ZB-2305; OriGene Technologies, Inc., Beijing, China) or anti-rabbit secondary antibodies (WLA023a; Wanleibio Co., Ltd.) for 60 min at 37˚C. After further washes with TBST, immunoreactive bands were visualized using an enhanced chemiluminescence detection system (Bio-Rad Laboratories, Inc., Hercules, CA, USA). Image Pro Plus 5 software (Bio-Rad Laboratories, Inc.) was used to semi-quantify the protein levels in each lane.

Statistical analysis. Experimental values are presented as the means ± standard deviation, and the difference between groups was analyzed by one-way analysis of variance with Tukey's and Newman Keuls post hoc tests. The experiments were conducted in triplicate. Statistical analysis was performed using SPSS 19.0 software (IBM Corp., Armonk, NY, USA). $P<0.05$ was considered to indicate a statistically significant difference.

Results

Characterization and differentiation of cultured MSCs. Surface molecular markers of MSCs were examined after 3-4 passages using flow cytometry. As shown in Fig. 1A, 96.84% of isolated cells expressed CD29. Conversely, few cells expressed the hematopoietic markers CD34 (1.33%) and CD45 (18.08%) (Fig. 1A and B). In addition, as shown in Fig. 1C and D, the cultured MSCs possessed the ability to differentiate along the osteogenic and adipogenic lineages, as determined by von Kossa and Oil Red O staining, respectively.

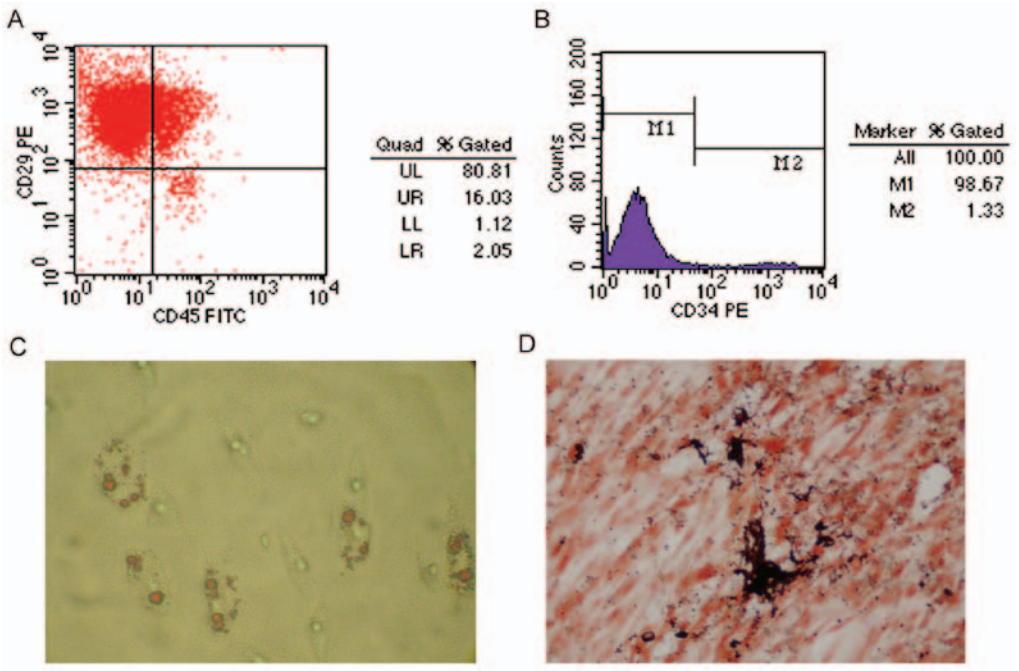

Figure 1. Characterization and differentiation of cultured MSCs. (A and B) Flow cytometric analysis of adherent, spindle-shaped MSCs (passage 3 or 4). Most cultured MSCs expressed CD29. However, the majority of MSCs were CD34- and CD45-negative. (C) Adiopogenic differentiation, as determined by Oil Red O staining. MSCs developed some lipid droplets (magnification, x400). (D) Osteogenic differentiation, as determined using von Kossa staining (magnification, x400). Mineralized matrix was formed in MSCs. CD, cluster of differentiation; FITC, fluorescein isothiocyanate; MSCs, mesenchymal stem cells; PE, phycoerythrin.

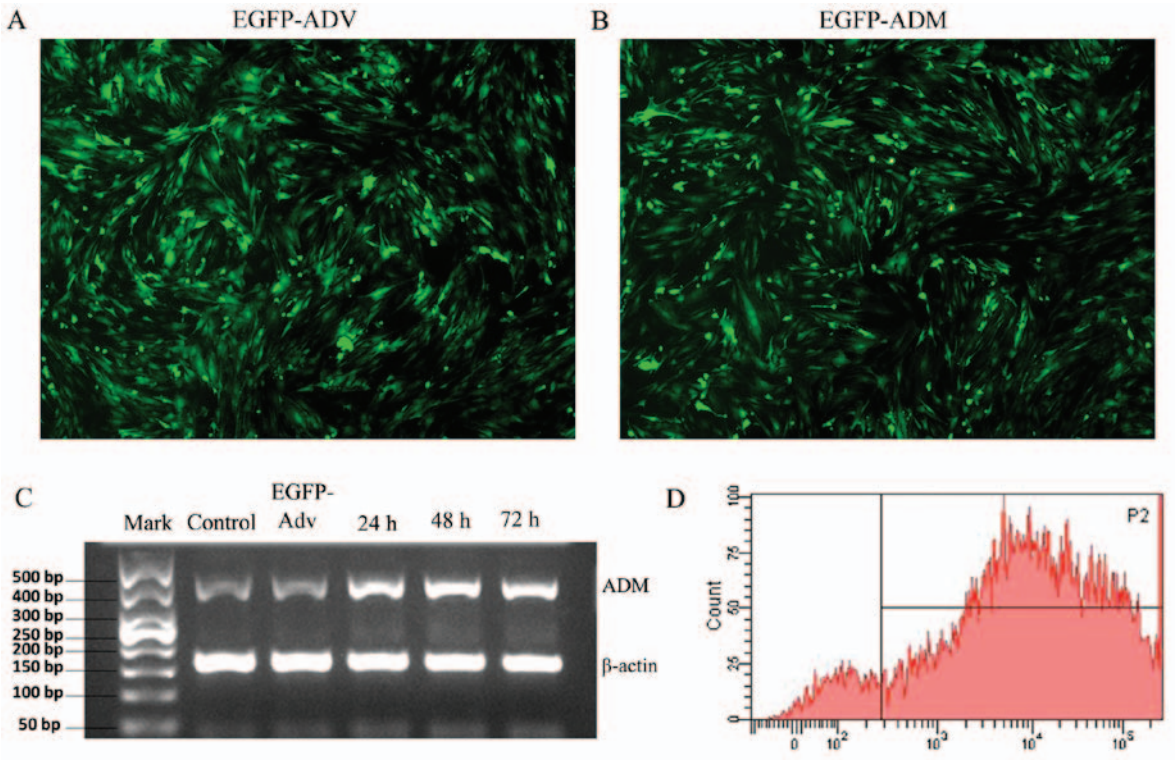

Figure 2. Infection of MSCs with adenovirus vectors. Fluorescence microscopy confirmed transduction efficiency in MSCs 48 h post-transduction with (A) EGFP-Adv or (B) EGFP-ADM (magnification, x100). (C) Representative reverse transcription-polymerase chain reaction results confirm ADM gene abundance following EGFP-ADM infection 24, 48 or 72 h post-transduction compared with in the control or EGFP-Adv groups. (D) Detection of transduction efficiency by flow cytometry. Adv, adenovirus; ADM, adrenomedullin; EGFP, enhanced green fluorescent protein; MSCs, mesenchymal stem cells.

EGFP-ADM infection increases the expression of ADM in MSCs. In the present study, infection efficiency was determined by detecting the positive rates of GFP fluorescence. Following infection with EGFP-Adv or EGFP-ADM for 48 h, ~100% of MSCs exhibited green fluorescence, which suggested that MSCs were successfully infected with the adenoviruses (Fig. 2A and B). Furthermore, to evaluate the mRNA expression levels of ADM in the genetically modified

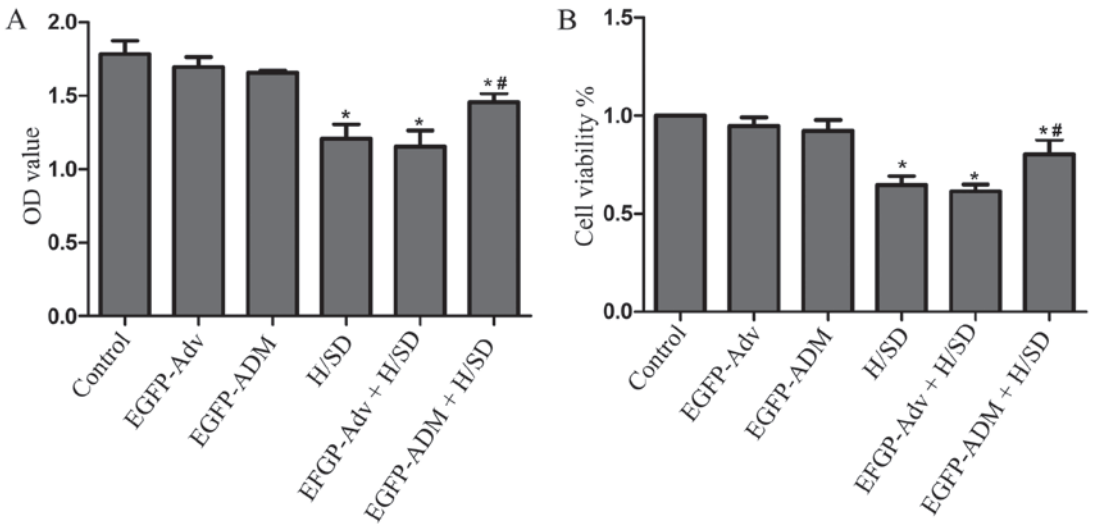

Figure 3. Effects of ADM on mesenchymal stem cell (A) proliferation and (B) viability. Data are presented as the means ± standard deviation of three independent experiments. *P<0.05 vs. the control group; #P<0.05 vs. the H/SD group. Adv, adenovirus; ADM, adrenomedullin; EGFP, enhanced green fluorescent protein; H/SD, hypoxia and serum deprivation; OD, optical denisty.

MSCs *in vitro*, RT-PCR analysis was performed on cell samples at 24, 48 and 72 h post-infection. The results demonstrated that the expression levels of ADM were markedly increased in the EGFP-ADM group as early as 24 h; the expression levels peaked at 48 h and were maintained until 72 h (Fig. 2C). Therefore, 48 h post-infection, the MSCs were used for subsequent experiments. Successful transduction at 48 h was also assessed by FACS analysis. As shown in Fig. 2D, >91% of MSCs were successfully transduced.

ADM increases MSC viability and proliferation. To investigate whether ADM protects MSCs against H/SD-induced injury, cell proliferation rate and viability rate were assessed using the CCK-8 assay. The cell viability rate was calculated using the following equation. Cell viability (%)=[OD (treated group) - A (blank)] / [OD (control) - OD (blank)] x100 The results detected no significant difference among the control (OD, 1.784±0.089; viability, 1±0), EGFP-Adv (OD, 1.696±0.066; viability, 0.947±0.036) and the EGFP-ADM-treated groups (OD, 1.656±0.015; viability, 0.923±0.046), thus indicating that adenovirus infection did not damage MSCs (Fig. 3). However, the proliferation and viability of MSCs was significantly decreased in the H/SD group (OD, 1.206±0.101; viability, 0.647±0.037) compared with in the control group (P<0.05). Conversely, the H/SD-induced impairments were markedly attenuated in the EGFP-ADM + H/SD group (OD, 1.457±0.062; viability, 0.802±0.061) compared with in the H/SD group (P<0.05), but not in the EGFP-Adv + H/SD group (OD, 1.154±0.109; viability, 0.615±0.028; P>0.05). These results suggested that ADM may protect MSCs against H/SD-induced injury (Fig. 3).

ADM protects MSCs from H/SD-induced apoptosis. DAPI and TUNEL staining were used to evaluate the protective effects of ADM on MSCs against H/SD-induced apoptosis. Briefly, modified or not modified MSCs were treated under H/SD conditions or normal conditions for 12 h; almost no TUNEL-positive cells were observed in the control (1.005±0.087), EGFP-ADM (1.179±0.165) and EGFP-Adv groups (1.091±0.079); however, cell shrinkage and nuclear condensation were markedly increased in the H/SD (6.683±0.178) and EGFP-Adv + H/SD groups (6.465±0.264) compared with in the control group (P<0.05), and no significant difference was detected between these two groups (P>0.05; Fig. 4). Notably, ADM transduction clearly exerted a protective effect on MSCs; the EGFP-ADM + H/SD group (3.428±0.229) possessed a significantly lower proportion of apoptotic cells compared with in the H/SD and EGFP-Adv + H/SD groups (P<0.05; Fig. 4).

In further studies, cell apoptosis was determined by flow cytometry. As shown in Fig. 5, the early apoptotic rate [Annexin V^+/AAD^-] was markedly increased in the H/SD (28.6±0.693) and EGFP-Adv + H/SD groups (29.667±1.857) compared with in the control (3.267±1.150; P<0.05), EGFP-ADM (3.433±1.709; P<0.05) and EGFP-Adv groups (3.067±1.266; P<0.05). In addition, there was no significant difference in the number of early apoptotic cells among the control, EGFP-ADM and EGFP-Adv groups (P>0.05). Notably, the EGFP-ADM + H/SD group (20.567±1.332) had a significantly lower proportion of cells in the early apoptotic phase compared with in the H/SD (P<0.05) and EGFP-Adv + H/SD groups (P<0.05); however, there were no differences in the number of cells in the late apoptotic phase (Annexin V^+/AAD^+) or necrosis (Annexin V^-/AAD^+) among the groups (data not shown). These findings indicated that overexpression of ADM in MSCs may protect against apoptosis under H/SD conditions.

Caspase-3 is a key effector protease associated with the execution of apoptosis. Under normal conditions, caspase-3 exists as inactivated procaspase-3. During apoptosis, procaspase-3 is activated and converted to cleaved caspase-3; therefore, the present study investigated the effects of ADM transduction on the expression of procaspase-3 and cleaved caspase-3. As shown in Fig. 6, the results demonstrated that the expression levels of cleaved caspase-3 were low in the control, EGFP-ADM and EGFP-Adv groups, according to the ratio of cleaved caspase-3/procaspase-3 (control, 0.361±0.134; EGFP-ADM group, 0.305±0.098; EGFP-Adv group, 0.348±0.103). Conversely, the ratio of cleaved

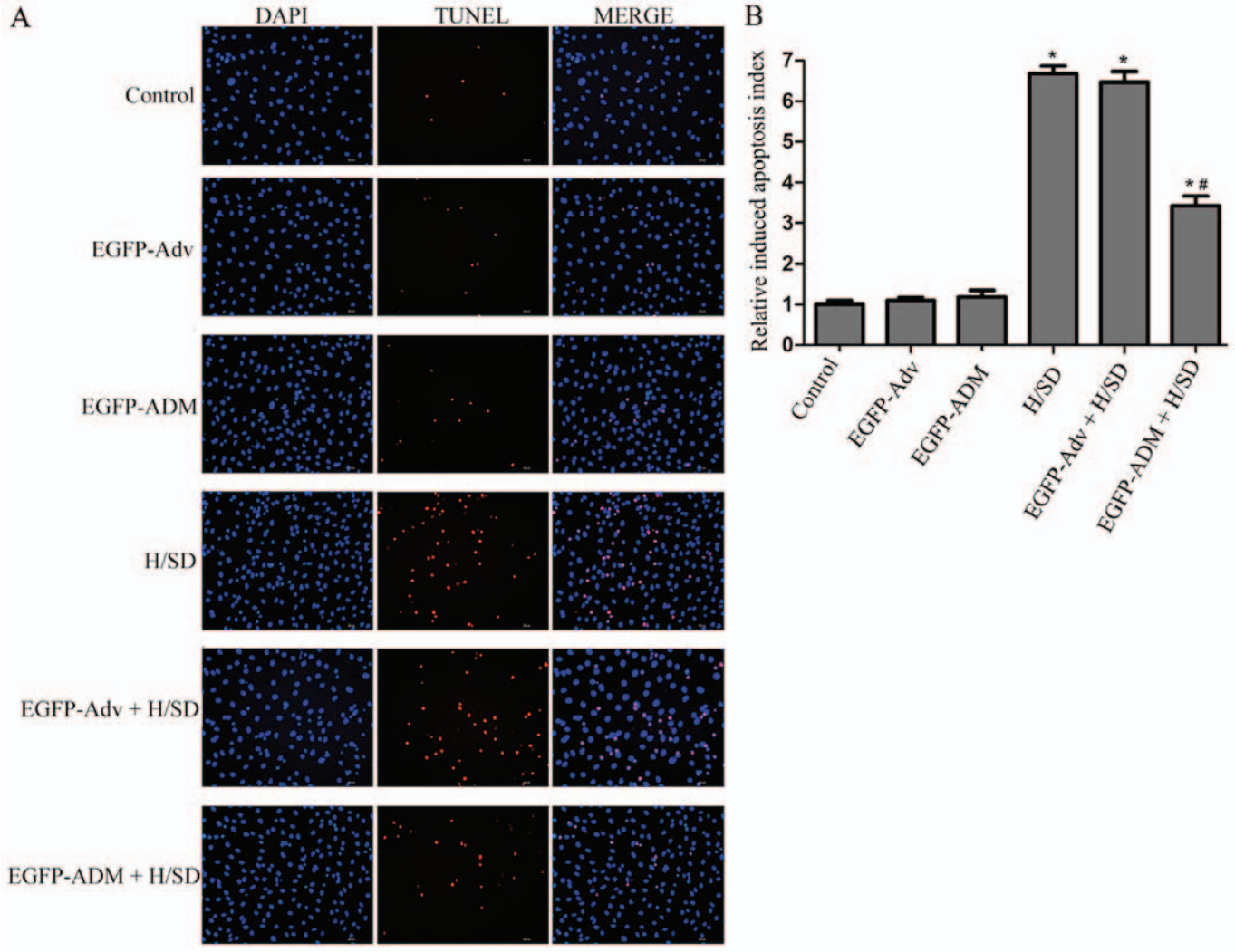

Figure 4. Apoptosis of MSCs induced by H/SD was measured by TUNEL staining. (A) Representative TUNEL staining of MSCs. Nuclear staining of red fluorescence was considered a positive apoptotic signal. DAPI served as a normal nuclear stain. The merge column presents an overlay of TUNEL and DAPI staining (magnification, x100). (B) Quantitative analysis of TUNEL staining. Data are presented as the means ± standard deviation of three independent experiments. *P<0.05 vs. the control group; #P<0.05 vs. the H/SD group. Adv, adenovirus; ADM, adrenomedullin; EGFP, enhanced green fluorescent protein; H/SD, hypoxia and serum deprivation; MSCs, mesenchymal stem cells; TUNEL, terminal deoxynucleotidyl transferase-mediated-dUTP nick-end labeling

caspase-3/procaspase-3 was markedly increased in the H/SD (0.829±0.144) and EGFP-Adv + H/SD groups (0.789±0.055) compared with in the control group (P<0.05). Furthermore, the present results demonstrated that this increase was attenuated in the EGFP-ADM + H/SD group (0.469±0.077) compared with in the vs. H/SD group (P<0.05). There was no significant difference between the EGFP-ADM + H/SD and control groups (P>0.05).

ADM prevents MSCs from H/SD-induced apoptosis via the Akt/GSK3β pathway. The present study investigated the mechanisms underlying the antiapoptotic effects of ADM. As aforementioned, the Akt/GSK3β pathway has been reported to be important in promoting survival in various cell systems. Therefore, the present study investigated whether this pathway may mediate the antiapoptotic effects of ADM in MSCs by western blot analysis. As shown in Fig. 7A and B, compared with in the control (1.027±0.056), EGFP-Adv (1.025±0.079) and EGFP-ADM (1.074±0.097) groups, the ratio of p-Akt/Akt was significantly decreased in the H/SD (0.462±0.089; P<0.05) and EGFP-Adv + H/SD groups (0.369±0.098; P<0.05). However, the ratio of p-Akt/Akt was markedly increased in the EGFP-ADM + H/SD group (0.958±0.039) compared with in the H/SD (P<0.05) and EGFP-Adv + H/SD groups (P<0.05). In addition, no obvious difference was detected among the control, EGFP-Adv and EGFP-ADM groups (P>0.05). GSK3β is an important downstream target of the Akt signaling pathway. Phosphorylation of GSK3β at the inactivating residue serine-9 by Akt results in GSK3β inactivation. Therefore, the present study investigated the effects of ADM on p-GSK3β expression. As shown in Fig. 7A and B, H/SD treatment (H/SD, 0.322±0.043; EGFP-Adv + H/SD, 0.389±0.053) decreased p-GSK3β expression compared with in the control (0.752±0.062; P<0.05), EGFP-Adv (0.829±0.034; P<0.05) and EGFP-ADM groups (0.708±0.035; P<0.05), whereas the expression levels of inactivated p-GSK3β were significantly enhanced in the EGFP-ADM + H/SD group (0.732±0.042) compared with in the H/SD group (P<0.05). There was no significant difference between the EGFP-ADM + H/SD and control groups (P>0.05).

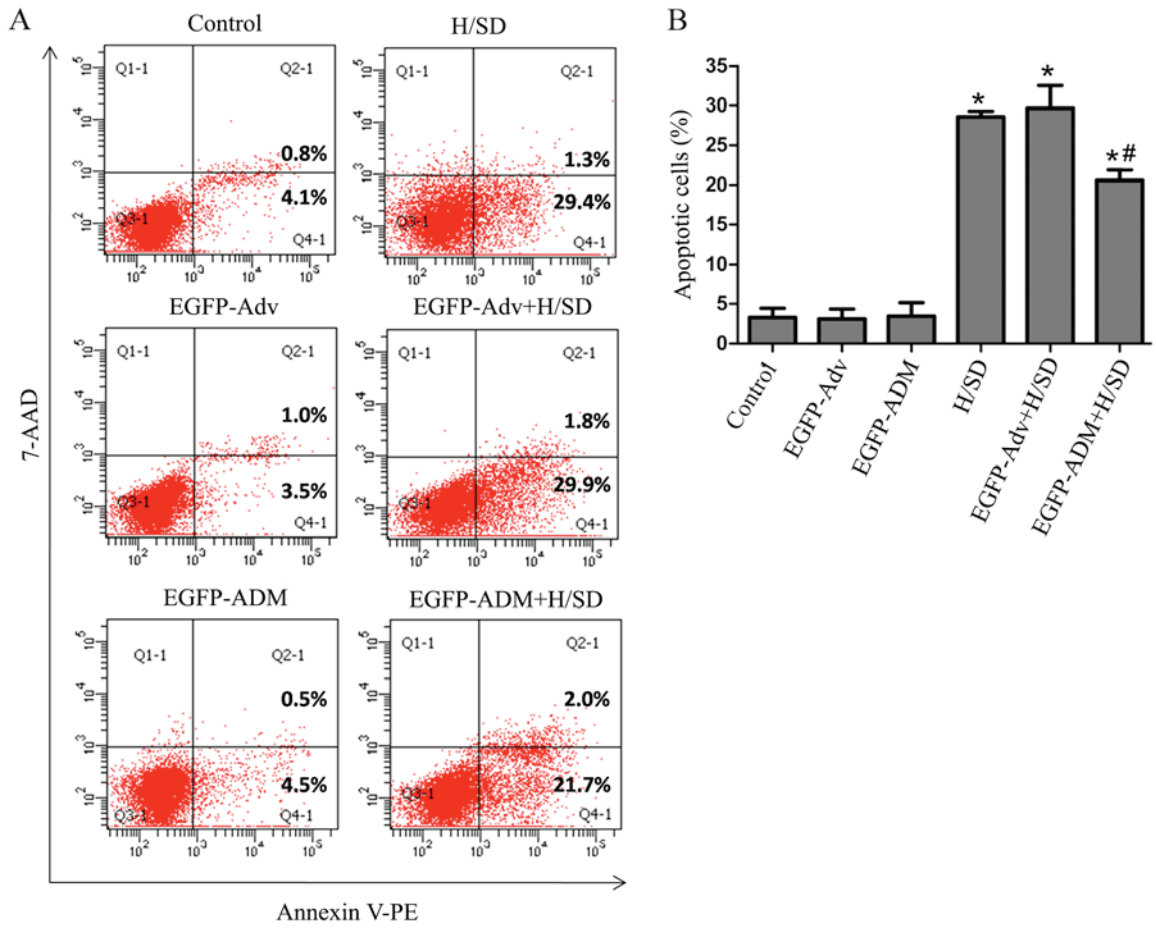

Figure 5. Apoptosis of mesenchymal stem cells was assessed by Annexin V/7-AAD double staining and FACS. (A) Representative FACS plots. (B) Quantitative analysis of the percentage of early-stage apoptotic cells (Annexin V^+/AAD^-). Data are presented as the means ± standard deviation from three independent experiments. *P<0.05 vs. the control group; #P<0.05 vs. the H/SD group. 7-AAD, 7-aminoactinomycin D; Adv, adenovirus; ADM, adrenomedullin; EGFP, enhanced green fluorescent protein; FACS, fluorescence-activated cell sorting; H/SD, hypoxia and serum deprivation; PE, phycoerythrin.

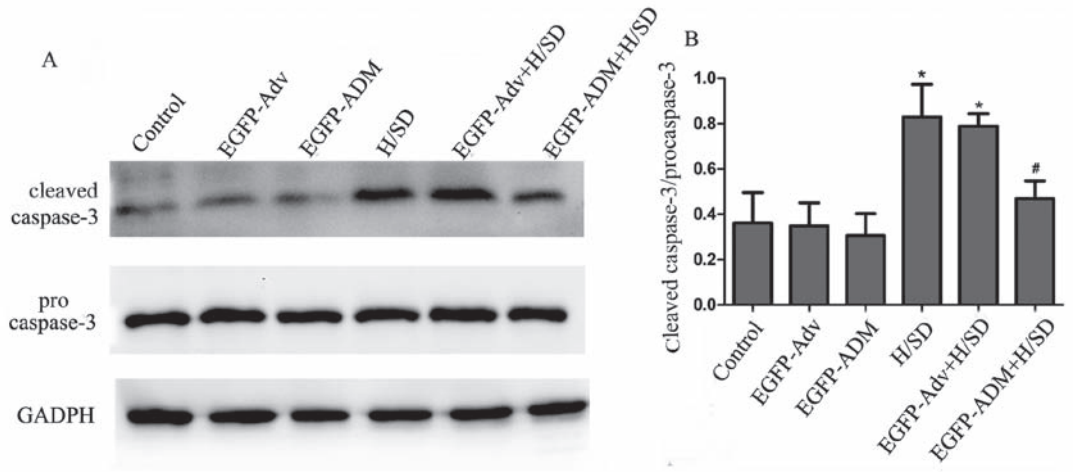

Figure 6. Effects of ADM on caspase-3 activition. (A) Representative western blot analyses of procaspase-3 and cleaved caspase-3 in the different groups. (B) Semi-quantitative analysis of the expression of cleaved caspase-3 was estimated as a fold-change relative to procaspase-3. Data are presented as the means ± standard deviation from three independent experiments. *P<0.05 vs. the control group; #P<0.05 vs. the H/SD group. Adv, adenovirus; ADM, adrenomedullin; EGFP, enhanced green fluorescent protein; H/SD, hypoxia and serum deprivation.

Antiapoptotic effects of ADM are involved in inhibition of the Bcl-2 pathway. Bcl-2 family members are important regulators of mitochondria-mediated apoptosis, and are classified as antiapoptotic proteins, such as Bcl-2, and proapoptotic proteins, such as Bax. The Bcl-2/Bax ratio is often used to determine the extent of apoptosis. The present results indicated that exposure of MSCs to H/SD conditions induced a significant decrease in the Bcl-2/Bax ratio (0.322±0.055)

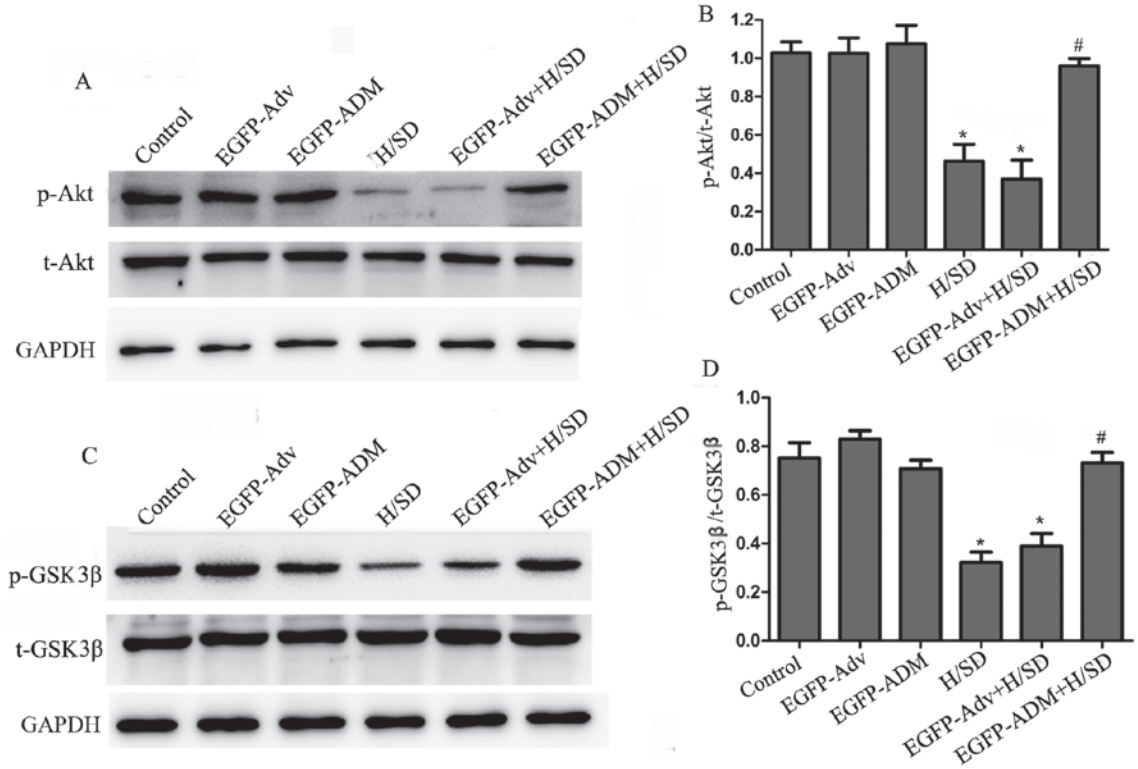

Figure 7. ADM activates the Akt/GSK3β pathway in the apoptosis of mesenchymal stem cells. (A) Representative western blot analyses of p-Akt and Akt. (B) Semi-quantitative analysis of the expression of p-Akt was estimated as a fold-change relative to Akt. (C) Representative western blot analyses of p-GSK3β and GSK3β. (D) Semi-quantitative analysis of the expression of p-GSK3β was estimated as a fold-change relative to GSK3β. Data are presented as the means ± standard deviation from three independent experiments. *P<0.05 vs. the control group; #P<0.05 vs. the H/SD group. Adv, adenovirus; ADM, adrenomedullin; Akt, protein kinase B; EGFP, enhanced green fluorescent protein; GSK3β, glycogen synthase kinase3β; H/SD, hypoxia and serum deprivation; p, phosphorylated; t, total.

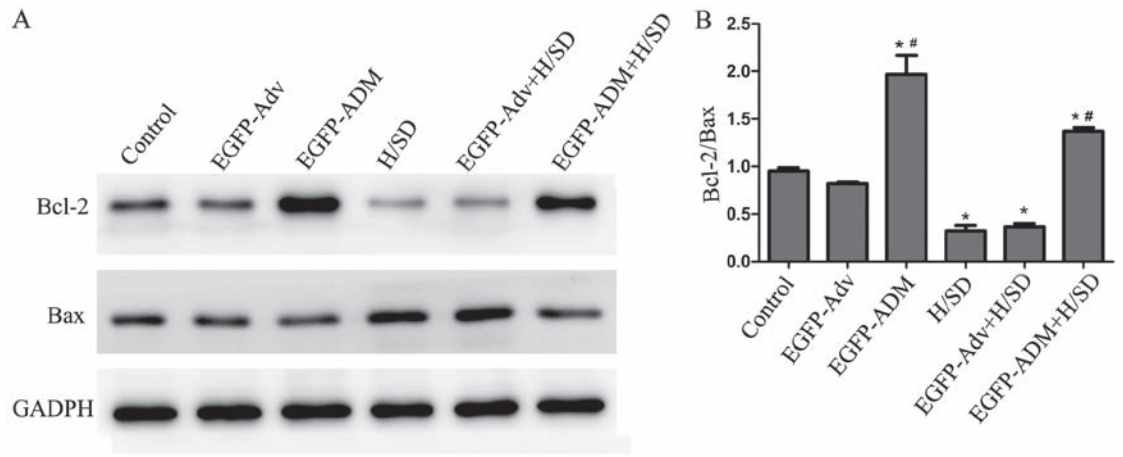

Figure 8. Effects of ADM on Bcl-2 and Bax expression. (A) Representative western blot analyses of Bcl-2, Bax and GADPH expression in the different groups. (B) Semi-quantitative analysis was used to calculate the relative ratio of Bcl-2/Bax. Data are presented as the means ± standard deviation from three independent experiments. *P<0.05 vs. the control group; #P<0.05 vs. the H/SD group. Adv, adenovirus; ADM, adrenomedullin; Bax, Bcl-2-associated X protein; Bcl-2, B-cell lymphoma 2; EGFP, enhanced green fluorescent protein; H/SD, hypoxia and serum deprivation.

compared with in the control (0.954±0.033; P<0.05) and EGFP-Adv + H/SD groups (0.364±0.035; P<0.05). Conversely, the Bcl-2/Bax ratio was significantly increased in the EGFP-ADM (1.967±0.201) and EGFP-ADM + H/SD groups (1.371±0.039) compared with in the control (P<0.05) and H/SD (P<0.05) groups (Fig. 8).

Discussion

The present study demonstrated that ADM overexpression exerted antiapoptotic effects on MSCs under H/SD conditions, and indicated that the protective effects were mediated via the Akt/GSK3β and Bcl-2 signaling pathways.

Due to the self-renewal ability, multi-directional differentiation potential and low immunogenicity of MSCs, and the ease with which they can be transfected/transduced in order to express heterologous genes, MSCs are considered an ideal choice to treat MI (29,34). However, previous studies reported that only 1-5% transplanted cells survive 48 h post-transplantation (7,8). In addition, three mechanisms have been reported to mediate cell death following transplantation, including nutrient and oxygen deprivation, inflammation, and a lack of matrix support and adhesion to extracellular matrix (35-38). The present study focused on one of these mechanisms, with the aim of increasing cell survival under conditions of nutrient and oxygen deprivation. Therefore, in the present study, a model of H/SD was used to induce apoptosis of MSCs *in vitro*. Similar to the findings of previous studies (10,28-30), the present results demonstrated that the apoptosis of MSCs was significantly increased under H/SD conditions, thus indicating that the H/SD model may successfully mimic the *in vivo* microenvironment of nutrient and oxygen deprivation in MI.

There are various strategies that may be used to overcome the low survival rates of transplanted cells. These approaches include pretreatment with growth factors or cytokines, preconditioning with hypoxia, and genetic modification to overexpress antideath or adhesion signals (35,36). The majority of preclinical and clinical gene therapy applications have used virus-based transfer of genetic material, due to high transduction efficiency, cell tropism and levels of transgene expression; however, detrimental immune reactions against the gene therapy vehicle, and transduced cells or transgene products, has raised important concerns (39). Therefore, it is desirable to develop an efficient and safe carrier for gene transfection. Jo *et al* reported that a non-viral carrier of cationized polysaccharide may be used for genetic engineering of MSCs, and indicated that it is a promising strategy to improve the therapeutic effects of MSCs (40). In addition, compared with direct adenovirus-injection as unbound adenovirus, recombinant adenovirus modification, which has been reported to have no major influence on the immunological properties of MSCs *in vitro* and *in vivo*, has been considered a suitable gene vector for therapeutic applications of MSCs and has been extensively used for the genetic modification of MSCs (41). Therefore, recombinant adenovirus modification was used in the present study. As expected, the present results demonstrated that the adenovirus itself did not harm MSCs with an MOI of 80, since there was no difference in MSC proliferation and viability among the control, EGFP-Adv and EGFP-ADM groups. Therefore, it was concluded that EGFP-ADM transduction is a safe and effective method to protect MSCs against H/SD-induced apoptosis. In the future, we aim to investigate more carriers for genetic engineering of MSCs.

ADM has been confirmed as a hypoxia-induced peptide, which is found in various human cancers, as well as in cell lines, where it serves an antiapoptotic role (18,42). Therefore, overexpression of ADM in MSCs was generated, in order to study its effect on the apoptosis of MSCs in the present study. The results demonstrated that gene modification with ADM could protect MSCs from H/SD-induced apoptosis, since apoptosis of MSCs was significantly decreased in the EGFP-ADM + H/SD group compared with in the H/SD and EGFP-Adv + H/SD groups.

The underlying mechanisms were subsequently investigated. Akt is a serine-threonine kinase, which has been reported to act as a powerful survival signal that exerts antiapoptotic effects and promotes cell survival. Akt can phosphorylate various transcription factors and other regulatory proteins. GSK3β is an important downstream signaling protein kinase of Akt. Phosphorylation of GSK3β at serine 9 leads to inhibition of its activity and reduces apoptosis (23-25,43,44). Furthermore, Yin *et al* demonstrated that ADM could protect cardiomyocytes against ischemia/reperfusion injury-induced apoptosis via the Akt-GSK-caspase signaling pathway in a rat model (19). Based on these findings, it may be hypothesized that ADM exerts protective effects on MSCs under H/SD conditions via the Akt/GSK3β pathway. Therefore, in the present study, the phosphorylation of Akt and GSK3β were detected by western blotting. The results clearly indicated that H/SD successfully induced MSC apoptosis and decreased the expression of p-Akt and p-GSK3β, whereas pretreatment with EGFP-ADM attenuated the apoptosis of MSCs and increased the expression levels of p-Akt and p-GSK3β. Therefore, it may be concluded that ADM gene transduction protects MSCs against H/SD-induced apoptosis through the Akt/GSK3β pathway. Caspase-3 acts as a key effector of apoptosis. Under normal conditions, it is initially synthesized as inactive precursors. During the final step of the proapoptotic signaling pathway in numerous cell lines, caspase-3 is activated to form cleaved caspase-3. Cleaved caspase-3 is a crucial downstream factor within the apoptotic cascade, which functions as an important executor of apoptosis (45). The present results revealed that cleaved caspase-3 was markedly increased in the H/SD group compared with in the control group; however, this increase was attenuated in the EGFP-ADM + H/SD group compared with in the EGFP-Adv + H/SD group, thus indicating that ADM may protect MSCs through reducing the activation of caspase-3.

Proteins in the Bcl-2 family serve an instrumental role in regulating apoptosis by controlling mitochondrial permeability and the release of cytochrome *c*. This protein family includes antiapoptotic proteins, including Bcl-2 and Bcl-extra large (xL), and proapoptotic proteins, such as Bcl-2-associated death promoter (Bad), BH3 interacting-domain death agonist, Bax and Bcl-2-like protein 11. Bcl-2 resides in the outer mitochondrial wall, maintains membrane integrity and inhibits cytochrome *c* release. Conversely, Bax resides in the cytosol but translocates to the mitochondria following death signaling, where it damages membrane integrity and promotes release of cytochrome *c*. The Bcl-2/Bax ratio is often adopted to represent the extent of apoptosis (12). Furthermore, Bcl-2 family proteins have been reported to be associated with Akt/GSK3β. Bad is a well known substrate of Akt. In addition, p-Akt and p-GSK3β have been reported to upregulate the expression of Bcl-2 and Bcl-xL, and increase the Bcl-2/Bax ratio (46,47). Zhou *et al* confirmed that early administration of ADM significantly reduced apoptosis of vascular endothelial cells, increased Bcl-2 protein levels and decreased Bax gene expression (48). Therefore, the present study further examined whether the Bcl-2 pathway was also involved in the antiapoptotic activity of ADM. In the present study, the protein expression levels of Bcl-2 and Bax were detected. Notably, the present results demonstrated that ADM increased Bcl-2 protein expression and improved the Bcl-2/Bax ratio, regardless of hypoxic or normoxic conditions. Furthermore,

although ADM could increase Bcl-2 protein expression under basal conditions, no effect was observed on the apoptotic rate between the control and EGFP-ADM groups, due to the low basal levels of apoptosis in MSCs. However, further investigation is required to elucidate the mechanisms underlying the effects of ADM on the increased expression of Bcl-2.

In conclusion, the results of the present study provided evidence to suggest that ADM promotes MSC survival under conditions mimicking myocardial ischemia. The prosurvival effects of ADM against H/SD-induced apoptosis may be mediated via the Akt/GSK3β and Bcl-2 signaling pathways.

Acknowledgements

The authors would like to thank Dr Wei Liu for her expert assistance with cell culture and western blot analysis. Dr Wei Liu is a member of the Key Laboratory of Myocardial Ischemia Mechanism and Treatment (Harbin Medical University), Ministry of Education (Harbin, China).

Funding

The present study was supported by grants from the Natural Science Foundation of Heilongjiang Province (grant no. QC2013C108), the Key Laboratory of Myocardial Ischemia, Harbin Medical University, Ministry of Education (grant no. KF201313) and the National Nature Science Foundations of China (grant no. 81700234).

Availability of data and materials

The datasets used and/or analyzed during the current study are available from the corresponding author on reasonable request.

Authors' contributions

LL conceived and designed the experiments. HS and YZ performed the experiments. YS analyzed the data. LL and HS wrote the paper.

Ethics approval and consent to participate

The present study was approved by the Local Ethics Committee for the Care and Use of Laboratory Animals of Harbin Medical University.

Consent for publication

Not applicable.

Competing interests

The authors declare that they have no competing interests.

References

1. Rouhi L, Kajbafzadeh AM, Modaresi M, Shariati M and Hamrahi D: Autologous serum enhances cardiomyocyte differentiation of rat bone marrow mesenchymal stem cells in the presence of transforming growth factor-β1 (TGF-β1). In Vitro Cell Dev Biol Anim 49: 287-294, 2013.
2. Ishimine H, Yamakawa N, Sasao M, Tadokoro M, Kami D, Komazaki S, Tokuhara M, Takada H, Ito Y, Kuno S, *et al*: N-Cadherin is a prospective cell surface marker of human mesenchymal stem cells that have high ability for cardiomyocyte differentiation. Biochem Biophys Res Commun 438: 753-759, 2013.
3. Fukuda K and Fujita J: Mesenchymal, but not hematopoietic, stem cells can be mobilized and differentiate into cardiomyocytes after myocardial infarction in mice. Kidney Int 68: 1940-1943, 2005.
4. Montanari S, Dayan V, Yannarelli G, Billia F, Viswanathan S, Connelly KA and Keating A: Mesenchymal stromal cells improve cardiac function and left ventricular remodeling in a heart transplantation model. J Heart Lung Transplant 34: 1481-1488, 2015.
5. Mathiasen AB, Qayyum AA, Jørgensen E, Helqvist S, Fischer-Nielsen A, Kofoed KF, Haack-Sørensen M, Ekblond A and Kastrup J: Bone marrow-derived mesenchymal stromal cell treatment in patients with severe ischaemic heart failure: A randomized placebo-controlled trial (MSC-HF trial). Eur Heart J 36: 1744-1753, 2015.
6. Mias C, Lairez O, Trouche E, Roncalli J, Calise D, Seguelas MH, Ordener C, Piercecchi-Marti MD, Auge N, Salvayre AN, *et al*: Mesenchymal stem cells promote matrix metalloproteinase secretion by cardiac fibroblasts and reduce cardiac ventricular fibrosis after myocardial infarction. Stem Cells 27: 2734-2743, 2009.
7. Müller-Ehmsen J, Krausgrill B, Burst V, Schenk K, Neisen UC, Fries JW, Fleischmann BK, Hescheler J and Schwinger RH: Effective engraftment but poor mid-term persistence of mononuclear and mesenchymal bone marrow cells in acute and chronic rat myocardial infarction. J Mol Cell Cardiol 41: 876-884, 2006.
8. Kolossov E, Bostani T, Roell W, Breitbach M, Pillekamp F, Nygren JM, Sasse P, Rubenchik O, Fries JW, Wenzel D, *et al*: Engraftment of engineered ES cell-derived cardiomyocytes but not BM cells restores contractile function to the infarcted myocardium. J Exp Med 203: 2315-2327, 2006.
9. Toma C, Pittenger MF, Cahill KS, Byrne BJ and Kessler PD: Human mesenchymal stem cells differentiate to a cardiomyocyte phenotype in the adult murine heart. Circulation 105: 93-98, 2002.
10. Zhu W, Chen J, Cong X, Hu S and Chen X: Hypoxia and serum deprivation-induced apoptosis in mesenchymal stem cells. Stem Cells 24: 416-425, 2006.
11. Suresh SC, Selvaraju V, Thirunavukkarasu M, Goldman JW, Husain A, Alexander Palesty J, Sanchez JA, McFadden DW and Maulik N: Thioredoxin-1 (Trx1) engineered mesenchymal stem cell therapy increased pro-angiogenic factors, reduced fibrosis and improved heart function in the infarcted rat myocardium. Int J Cardiol 201: 517-528, 2015.
12. Wu XY, Hao CP, Ling M, Guo CH and Ma W: Hypoxia-induced apoptosis is blocked by adrenomedullin via upregulation of Bcl-2 in human osteosarcoma cells. Oncol Rep 34: 787-794, 2015.
13. Di Liddo R, Bridi D, Gottardi M, De Angeli S, Grandi C, Tasso A, Bertalot T, Martinelli G, Gherlinzoni F and Conconi MT: Adrenomedullin in the growth modulation and differentiation of acute myeloid leukemia cells. Int J Oncol 48: 1659-1669, 2016.
14. Ah Kioon MD, Asensio C, Ea HK, Velard F, Uzan B, Rullé S, Bazille C, Marty C, Falgarone G, Nguyen C, *et al*: Adrenomedullin(22-52) combats inflammation and prevents systemic bone loss in murine collagen-induced arthritis. Arthritis Rheum 64: 1069-1081, 2012.
15. Kaafarani I, Fernandez-Sauze S, Berenguer C, Chinot O, Delfino C, Dussert C, Metellus P, Boudouresque F, Mabrouk K, Grisoli F, *et al*: Targeting adrenomedullin receptors with systemic delivery of neutralizing antibodies inhibits tumor angiogenesis and suppresses growth of human tumor xenografts in mice. FASEB J 23: 3424-3435, 2009.
16. Chen P, Huang Y, Bong R, Ding Y, Song N, Wang X, Song X and Luo Y: Tumor-associated macrophages promote angiogenesis and melanoma growth via adrenomedullin in a paracrine and autocrine manner. Clin Cancer Res 17: 7230-7239, 2011.
17. Sakimoto S, Kidoya H, Kamei M, Naito H, Yamakawa D, Sakaguchi H, Wakabayashi T, Nishida K and Takakura N: An angiogenic role for adrenomedullin in choroidal neovascularization. PLoS One 8: e58096, 2013.
18. Kim JY, Park WD, Lee S and Park JH: Adrenomedullin is involved in the progression of colonic adenocarcinoma. Mol Med Rep 6: 1030-1034, 2012.

19. Yin H, Chao L and Chao J: Adrenomedullin protects against myocardial apoptosis after ischemia/reperfusion through activation of Akt-GSK signaling. Hypertension 43: 109-116, 2004.
20. Zhou PH, Hu W and Zhang XB: Wang W2, Zhang LJ: Protective effect of adrenomedullin on rat leydig cells from lipopolysaccharide-induced inflammation and apoptosis via the PI3K/Akt signaling pathway ADM on rat leydig cells from inflammation and apoptosis. Mediators Inflamm 2016: 7201549, , 2016.
21. Kong XQ, Wang LX, Yang CS, Chen SF, Xue YZ and Liu YH: Effects of adrenomedullin on the cell numbers and apoptosis of endothelial progenitor cells. Clin Invest Med 31: E117-E122, 2008.
22. Kim W, Moon SO, Sung MJ, Kim SH, Lee S, Kim HJ, Koh GY and Park SK: Protective effect of adrenomedullin in mannitol-induced apoptosis. Apoptosis 7: 527-536, 2002.
23. Chen L, Zhang Y, Sun X, Li H, LeSage G, Javer A, Zhang X, Wei X, Jiang Y and Yin D: Synthetic resveratrol aliphatic acid inhibits TLR2-mediated apoptosis and an involvement of Akt/GSK3β pathway. Bioorg Med Chem 17: 4378-4382, 2009.
24. Ying Y, Zhu H, Liang Z, Ma X and Li S: GLP1 protects cardiomyocytes from palmitate-induced apoptosis via Akt/GSK3b/b-catenin pathway. J Mol Endocrinol 55: 245-262, 2015.
25. Yin H, Chao L and Chao J: Kallikrein/kinin protects against myocardial apoptosis after ischemia/reperfusion via Akt-glycogen synthase kinase-3 and Akt-Bad.14-3-3 signaling pathways. J Biol Chem 280: 8022-8030, 2005.
26. Kim CH, Hao J, Ahn HY and Kim SW: Activation of Akt/protein kinase B mediates the protective effects of mechanical stretching against myocardial ischemia-reperfusion injury. J Vet Sci 13: 235-244, 2012.
27. Song JQ, Teng X, Cai Y, Tang CS and Qi YF: Activation of Akt/GSK-3β signaling pathway is involved in intermedin(1-53) protection against myocardial apoptosis induced by ischemia/reperfusion. Apoptosis 14: 1061-1069, 2009.
28. Chen J, Baydoun AR, Xu R, Deng L, Liu X, Zhu W, Shi L, Cong X, Hu S and Chen X: Lysophosphatidic acid protects mesenchymal stem cells against hypoxia and serum deprivation-induced apoptosis. Stem Cells 26: 135-145, 2008.
29. He J, Wang C, Sun Y, Lu B, Cui J, Dong N, Zhang M, Liu Y and Yu B: Exendin-4 protects bone marrow-derived mesenchymal stem cells against oxygen/glucose and serum deprivation-induced apoptosis through the activation of the cAMP/PKA signaling pathway and the attenuation of ER stress. Int J Mol Med 37: 889-900, 2016.
30. Zhang F, Cui J, Lv B and Yu B: Nicorandil protects mesenchymal stem cells against hypoxia and serum deprivation-induced apoptosis. Int J Mol Med 36: 415-423, 2015.
31. Li L, Zhang S, Zhang Y, Yu B, Xu Y and Guan Z: Paracrine action mediate the antifibrotic effect of transplanted mesenchymal stem cells in a rat model of global heart failure. Mol Biol Rep 36: 725-731, 2009.
32. Zhu X, Jiang Y, Shan PF, Shen J, Liang QH, Cui RR, Liu Y, Liu GY, Wu SS, Lu Q, *et al*: Vaspin attenuates the apoptosis of human osteoblasts through ERK signaling pathway. Amino Acids 44: 961-968, 2013.
33. Yu D, Mu S, Zhao D, Wang G, Chen Z, Ren H and Fu Q: Puerarin attenuates glucocorticoid-induced apoptosis of hFOB1.19 cells through the JNK- and Akt-mediated mitochondrial apoptotic pathways. Int J Mol Med 36: 345-354, 2015.
34. Parekkadan B and Milwid JM: Mesenchymal stem cells as therapeutics. Annu Rev Biomed Eng 12: 87-117, 2010.
35. Shi RZ and Li QP: Improving outcome of transplanted mesenchymal stem cells for ischemic heart disease. Biochem Biophys Res Commun 376: 247-250, 2008.
36. Robey TE, Saiget MK, Reinecke H and Murry CE: Systems approaches to preventing transplanted cell death in cardiac repair. J Mol Cell Cardiol 45: 567-581, 2008.
37. Amiri F, Jahanian-Najafabadi A and Roudkenar MH: In vitro augmentation of mesenchymal stem cells viability in stressful microenvironments: In vitro augmentation of mesenchymal stem cells viability. Cell Stress Chaperones 20: 237-251, 2015.
38. Potier E, Ferreira E, Meunier A, Sedel L, Logeart-Avramoglou D and Petite H: Prolonged hypoxia concomitant with serum deprivation induces massive human mesenchymal stem cell death. Tissue Eng 13: 1325-1331, 2007.
39. Edelstein ML, Abedi MR and Wixon J: Gene therapy clinical trials worldwide to 2007 - an update. J Gene Med 9: 833-842, 2007.
40. Jo J, Nagaya N, Miyahara Y, Kataoka M, Harada-Shiba M, Kangawa K and Tabata Y: Transplantation of genetically engineered mesenchymal stem cells improves cardiac function in rats with myocardial infarction: Benefit of a novel nonviral vector, cationized dextran. Tissue Eng 13: 313-322, 2007.
41. Treacy O, Ryan AE, Heinzl T, O'Flynn L, Cregg M, Wilk M, Odoardi F, Lohan P, O'Brien T, Nosov M, *et al*: Adenoviral transduction of mesenchymal stem cells: In vitro responses and in vivo immune responses after cell transplantation. PLoS One 7: e42662, 2012.
42. Park SC, Yoon JH, Lee JH, Yu SJ, Myung SJ, Kim W, Gwak GY, Lee SH, Lee SM, Jang JJ, *et al*: Hypoxia-inducible adrenomedullin accelerates hepatocellular carcinoma cell growth. Cancer Lett 271: 314-322, 2008.
43. Chung H, Seo S, Moon M and Park S: Phosphatidylinositol-3-kinase/Akt/glycogen synthase kinase-3 beta and ERK1/2 pathways mediate protective effects of acylated and unacylated ghrelin against oxygen-glucose deprivation-induced apoptosis in primary rat cortical neuronal cells. J Endocrinol 198: 511-521, 2008.
44. Yan X, Lyu T, Jia N, Yu Y, Hua K and Feng W: Huaier aqueous extract inhibits ovarian cancer cell motility via the AKT/GSK3β/β-catenin pathway. PLoS One 8: e63731, 2013.
45. Porter AG and Jänicke RU: Emerging roles of caspase-3 in apoptosis. Cell Death Differ 6: 99-104, 1999.
46. Linseman DA, Butts BD, Precht TA, Phelps RA, Le SS, Laessig TA, Bouchard RJ, Florez-McClure ML and Heidenreich KA: Glycogen synthase kinase-3beta phosphorylates Bax and promotes its mitochondrial localization during neuronal apoptosis. J Neurosci 24: 9993-10002, 2004.
47. Kaga S, Zhan L, Altaf E and Maulik N: Glycogen synthase kinase-3beta/beta-catenin promotes angiogenic and anti-apoptotic signaling through the induction of VEGF, Bcl-2 and survivin expression in rat ischemic preconditioned myocardium. J Mol Cell Cardiol 40: 138-147, 2006.
48. Zhou M, Simms HH and Wang P: Adrenomedullin and adrenomedullin binding protein-1 attenuate vascular endothelial cell apoptosis in sepsis. Ann Surg 240: 321-330, 2004.